

**Motion induced excitation and radiation from an atom facing a mirror**César D. Fosco,<sup>1,\*</sup> Fernando C. Lombardo<sup>2,†</sup> and Francisco D. Mazzitelli<sup>1,‡</sup><sup>1</sup>*Centro Atómico Bariloche and Instituto Balseiro, Comisión Nacional de Energía Atómica, R8402AGP Bariloche, Argentina*<sup>2</sup>*Departamento de Física Juan José Giambiagi, FCEyN UBA, Facultad de Ciencias Exactas y Naturales, Ciudad Universitaria, Pabellón I, 1428 Buenos Aires, Argentina*

(Received 4 January 2022; accepted 11 February 2022; published 23 February 2022)

We study quantum dissipative effects due to the nonrelativistic, bounded, accelerated motion of a single neutral atom in the presence of a planar perfect mirror, i.e., a perfect conductor at all frequencies. We consider a simplified model whereby a moving “scalar atom” is coupled to a quantum real scalar field, subjected to either Dirichlet or Neumann boundary conditions on the plane. We use an expansion in powers of the departure of the atom with respect to a static average position to compute the vacuum persistence amplitude and the resulting vacuum decay probability. We evaluate transition amplitudes corresponding to the excitation of the atom plus the emission of a particle, and show explicitly that the vacuum decay probabilities match the results obtained by integrating the transition amplitudes over the directions of the emitted particle. We also compute the spontaneous emission rate of an oscillating atom that is initially in an excited state.

DOI: [10.1103/PhysRevD.105.045019](https://doi.org/10.1103/PhysRevD.105.045019)**I. INTRODUCTION**

Quantum vacuum fluctuations are at the origin of many interesting phenomena. A prominent place among them corresponds to the forces arising between static neutral objects, originated in the fluctuations of the electromagnetic (EM) field. These Casimir forces [1] have been measured with precision in the last decades, and there have also been theoretical advances on finding their dependence on the geometry and composition of the bodies.

Vacuum fluctuations also affect the decay probability of single atoms, via spontaneous emission. In the proximity of metallic plates or when the atom is in a cavity, those decay probabilities may change because of the influence of the boundary conditions on the properties of those fluctuations. This kind of effect has been investigated in the context of cavity electrodynamics [2].

Qualitatively different effects appear when the system is subjected to time dependent external conditions; for example, photon creation when macroscopic media are accelerated or when, being static, a time dependence of their electromagnetic properties is induced. Moreover (under some conditions) even for a medium that moves at a constant velocity with respect to a static one, a frictional force, termed “quantum friction,” may arise. These phenomena, broadly named dynamical Casimir effect [3], do also manifest themselves at a microscopic level.

For example, the oscillatory motion of the center of mass of an atom, which is initially in its ground state, can lead to different excited states of the atom-field system: one of them corresponds to a final state where the atom itself has been excited, and a photon has been emitted. Alternatively, the final state may contain a pair of photons, with the atom still in its ground state. The latter is the microscopic counterpart of the photon-creation process due to a moving mirror [4]. A different mechanism, not involving motion, arises when external driving fields produce a time dependence in the energy levels [5].

Another interesting line of research, closely related to the present paper, focuses on single atoms near a mirror, and in relative motion to it. For example, for a two level atom in its excited state, an oscillating mirror induces modifications in the decay probability and in the spectrum of the emitted photons [6,7]. Oscillating atoms near a perfect mirror have been considered in a number of situations, most of them using simplifying assumptions, either about the direction of the emitted photons [8,9] or considering a scalar rather than the EM field [10]. For uniform acceleration, the relation between the excitation probability for a moving atom has been compared with that of a moving mirror in discussions of the equivalence principle [9]. Imperfect mirrors have also been considered, in particular, in our previous work [11] on quantum dissipative effects for an atom moving nonrelativistically in the presence of a graphene sheet. The calculations were performed perturbatively in the coupling constants that define the imperfect media, estimating the dissipative phenomena, in this context, via the imaginary

\*fosco@cab.cnea.gov.ar

†lombardo@df.uba.ar

‡fdmazzi@cab.cnea.gov.ar

part of the in-out effective action. This is a “global” observable, namely, it accounts for the total probability of vacuum decay.

In this paper, and for a similar kind of system, we present a twofold approach to study quantum dissipation and then check their consistency: we first evaluate the imaginary part of the effective action, and then present a more refined study, by evaluating the probability of photon emission as a function of the direction of the emitted photons. The consistency of both approaches is checked by integrating out that emission probability over all the possible angles, and comparing with the probability of vacuum decay. We also consider the case of a moving atom that is initially in an excited state, and analyze the dependence of the probability of spontaneous emission on the acceleration of the atom and its distance to the mirror. We have done all calculations for a model where a real scalar field couples to a scalar model for an atom, which moves in the presence of a “perfect” mirror; namely, one which imposes either Dirichlet or Neumann boundary conditions.

This paper is organized as follows: in Sec. II, we introduce the model and evaluate the imaginary part of its effective action, both for Dirichlet and Neumann boundary conditions, to the second order in the amplitude of motion of the atom. In Sec. III, we evaluate the transition probabilities. We find the total decay probability and also show its consistency with the finer description of the elementary processes of photon emission and atom excitation. We also discuss the decay or spontaneous emission process in terms of its corresponding probability. Finally, in Sec. IV, we summarize our main conclusions.

## II. THE EFFECTIVE ACTION

It has become common usage in research related to both the static and dynamic Casimir effects to begin the analysis of the phenomenon being studied in a simplified setting, with a real scalar field playing the role of the full EM field. In some cases, one can even show that transverse electric and transverse magnetic modes can be described by scalar fields satisfying either Dirichlet and Neumann boundary conditions, and that the EM field results may be obtained as the superposition of those two scalar field theories.

In our model, an atom will be coupled to a quantum real scalar field, and we will assume “perfect” boundary conditions for the scalar field on the flat boundary, i.e., Dirichlet or Neumann. The free action for the massless scalar field shall be given by

$$\mathcal{S}_{\text{sc}}(\phi) = \frac{1}{2} \int d^4x \partial_\mu \phi(x) \partial^\mu \phi(x), \quad (1)$$

and boundary conditions will be assumed to be implemented at the level of the functional integral over gauge field fluctuations. In our conventions, indices from the middle of the Roman alphabet ( $i, j, \dots$ ) are assumed to run

from 1 to 3, while those of the middle of the Greek alphabet ( $\mu, \nu, \dots$ ) run from 0 to 3, with  $x^0 \equiv ct$ . In our conventions,  $c \equiv 1$ . The metric tensor is, on the other hand, assumed to be  $(g_{\mu\nu}) = \text{diag}(1, -1, -1, -1)$ . Einstein convention on the sum over repeated indices is also understood, unless explicitly stated otherwise.

The classical action for the atom is, on the other hand, assumed to be

$$\mathcal{S}_a = \frac{m}{2} \int dt (\dot{q}^2 - \Omega^2 q^2) + g \int dt q(t) \phi(t, \mathbf{r}(t)), \quad (2)$$

where  $q(t)$  plays the role of the electron’s degree of freedom,  $\mathbf{r}(t)$  of the atom’s center of mass,  $m$  is the electron’s mass, and  $g$  is the coupling constant between the electron and the vacuum field. We will assume that the motion of the center of mass is bounded and we will denote by  $\mathbf{r}_0$  the (time) averaged position.

Following a similar approach to the one of our previous work [11], we first integrate out the internal degree of freedom  $q(t)$ , what produces an “intermediate” effective action  $\mathcal{S}_{\text{eff}}(\phi; \mathbf{r})$ , given by the following expression:

$$\mathcal{S}_{\text{eff}}(\phi; \mathbf{r}) = \mathcal{S}_{\text{sc}}(\phi) + \mathcal{S}_I^{(a)}(\phi; \mathbf{r}), \quad (3)$$

with

$$\mathcal{S}_I^{(a)}(\phi; \mathbf{r}) = -\frac{g^2}{2} \int dt \int dt' \Delta(t-t') \phi(t, \mathbf{r}(t)) \phi(t', \mathbf{r}(t')), \quad (4)$$

where  $\Delta(t-t') = \int \frac{d\nu}{2\pi} e^{-i\nu(t-t')} \tilde{\Delta}(\nu)$ , and

$$\tilde{\Delta}(\nu) = \frac{i}{m(\nu^2 - \Omega^2 + i\epsilon)}. \quad (5)$$

Then, the complete effective action of the system, functional of the center of mass coordinates,  $\Gamma[\mathbf{r}(t)]$ , is obtained by including the real scalar field fluctuations in the presence of the appropriate boundary conditions. Namely,

$$e^{i\Gamma[\mathbf{r}(t)]} = \frac{\int [\mathcal{D}\phi]_m e^{i\mathcal{S}_{\text{eff}}(\phi; \mathbf{r})}}{\int [\mathcal{D}\phi]_m e^{i\mathcal{S}_{\text{eff}}(\phi; \mathbf{r}_0)}}. \quad (6)$$

The subindex “ $m$ ” for the brackets in the field integration measure has been included to signal that the integral is over those field configurations that are compatible with the boundary conditions imposed by the mirrors. In our case, and as already advanced, those conditions will be either Dirichlet or Neumann on the plane  $x^3 = 0$ . We shall not need to actually perform the full integrals above when we evaluate  $\Gamma[\mathbf{r}(t)]$  to the first order in  $\mathcal{S}_I^{(a)}$ . Indeed, to that order, we just need the correlator of two fields in the presence of the mirror, which is just the field propagator in

the presence of Dirichlet or Neumann conditions on a plane. More explicitly, and denoting the contribution of first order in  $S_I^{(a)}$  by  $\Gamma^{(am)}[\mathbf{r}(t)]$ , we see that

$$\Gamma^{(am)}[\mathbf{r}(t)] = \frac{ie^2}{2} \int dt \int dt' \Delta(t-t') \times \langle \phi(t, \mathbf{r}(t)) \phi(t', \mathbf{r}(t')) \rangle^{(m)}, \quad (7)$$

where the symbol  $\langle \dots \rangle^{(m)}$  denotes the functional averaging

$$\langle \dots \rangle^{(m)} = \frac{\int [\mathcal{D}\phi]_m \dots e^{iS_{sc}(\phi)}}{\int [\mathcal{D}\phi]_m e^{iS_{sc}(\phi)}}. \quad (8)$$

### A. Dirichlet mirror

For a Dirichlet mirror, we can simply use the images method to write

$$\langle \phi(x) \phi(y) \rangle_m = G_0(x^0 - y^0, x^1 - y^1, x^2 - y^2, x^3 - y^3) - G_0(x^0 - y^0, x^1 - y^1, x^2 - y^2, x^3 + y^3), \quad (9)$$

where  $G_0$  is the free scalar-field propagator

$$G_0(x^0 - y^0, x^1 - y^1, x^2 - y^2, x^3 - y^3) = \int \frac{d^4 k}{(2\pi)^4} e^{-ik \cdot (x-y)} \frac{i}{k^2 + i\epsilon}. \quad (10)$$

Introducing the explicit form of the Dirichlet propagator above into (7), and using an entirely analogous approach to the one of [10] we obtain, after some algebra,

$$\begin{aligned} \text{Im}[\Gamma_{mp}^D] &= \frac{g^2}{8\Omega m} \int \frac{d^3 p}{(2\pi)^3} \frac{1}{p} \\ &\times [f(-\mathbf{p}_{\parallel}, -p^3, -(p + \Omega)) f(\mathbf{p}_{\parallel}, p^3, p + \Omega) \\ &- f(-\mathbf{p}_{\parallel}, p^3, -(p + \Omega)) f(\mathbf{p}_{\parallel}, p^3, p + \Omega)], \end{aligned} \quad (11)$$

where  $\mathbf{p} = (\mathbf{p}_{\parallel}, p^3)$ ,  $p = |\mathbf{p}|$ , and

$$f(\mathbf{p}, \nu) = \int_{-\infty}^{+\infty} dt e^{-i\mathbf{p} \cdot \mathbf{r}(t)} e^{i\nu t}. \quad (12)$$

We obtain more explicit expressions by expanding in powers of the departure of the atom from an equilibrium position  $\mathbf{r}_0$ , which in our choice of coordinates will be of the form  $\mathbf{r}_0 = (0, 0, a)$ ,  $a > 0$ .

To the second order in the departure, which we denote  $\mathbf{y}(t)$ , and using tildes to denote time Fourier transforms, we find

$$\text{Im}[\Gamma_{mp}^D] = \frac{1}{2} \int_{-\infty}^{+\infty} \frac{d\nu}{2\pi} \tilde{y}^i(-\nu) \tilde{y}^j(\nu) m_D^{ij}(\nu). \quad (13)$$

Because of the presence of the plate, spatial isotropy is lost and  $m_D^{ij}(\nu)$  and not proportional to  $\delta^{ij}$ . Rather, as a  $3 \times 3$  matrix, it has the form

$$[m_D^{ij}(\nu)] = \begin{pmatrix} m_{\parallel}(\nu) & 0 & 0 \\ 0 & m_{\parallel}(\nu) & 0 \\ 0 & 0 & m_{\perp}(\nu) \end{pmatrix}, \quad (14)$$

where the parallel component is

$$m_{\parallel}(\nu) = \frac{\pi g^2}{2m\Omega} \theta(|\nu| - \Omega) \int \frac{d^3 p}{(2\pi)^3} \frac{\mathbf{p}_{\parallel}^2}{2p} [1 - \cos(2p^3 a)] \times \delta(|\nu| - p - \Omega), \quad (15)$$

and results in

$$m_{\parallel}(\nu) = \frac{g^2}{8\pi m \Omega} \theta(|\nu| - \Omega) (|\nu| - \Omega)^3 \times \left\{ \frac{2}{3} + \frac{\cos(2(|\nu| - \Omega)a)}{2[(|\nu| - \Omega)a]^2} - \frac{\sin(2(|\nu| - \Omega)a)}{4[(|\nu| - \Omega)a]^3} \right\}. \quad (16)$$

The perpendicular component, on the other hand, is given by

$$m_{\perp}(\nu) = \frac{\pi g^2}{2m\Omega} \theta(|\nu| - \Omega) \int \frac{d^3 p}{(2\pi)^3} \frac{(p^3)^2}{p} [1 + \cos(2p^3 a)] \times \delta(|\nu| - p - \Omega), \quad (17)$$

or

$$m_{\perp}(\nu) = \frac{g^2}{4\pi m \Omega} \theta(|\nu| - \Omega) (|\nu| - \Omega)^3 \times \left\{ \frac{1}{3} + \frac{\cos(2(|\nu| - \Omega)a)}{2[(|\nu| - \Omega)a]^2} - \frac{\sin(2(|\nu| - \Omega)a)}{4[(|\nu| - \Omega)a]^3} + \frac{\sin(2(|\nu| - \Omega)a)}{2[(|\nu| - \Omega)a]} \right\}. \quad (18)$$

It can be seen that both functions,  $m_{\parallel}$  and  $m_{\perp}$  approach a common limit  $m_0$  far from the plate, i.e., when  $|\nu|a \rightarrow \infty$ :

$$m_0(\nu) = \frac{g^2}{12\pi m \Omega} \Theta(|\nu| - \Omega) (|\nu| - \Omega)^3. \quad (19)$$

As expected, this is the result corresponding to an oscillating atom in free space [10]. In Fig. 1 we plot the ratios  $m_{\perp}/m_0$  and  $m_{\parallel}/m_0$  as functions of  $a(|\nu| - \Omega)$ , where the above mentioned limit can be seen explicitly. On the

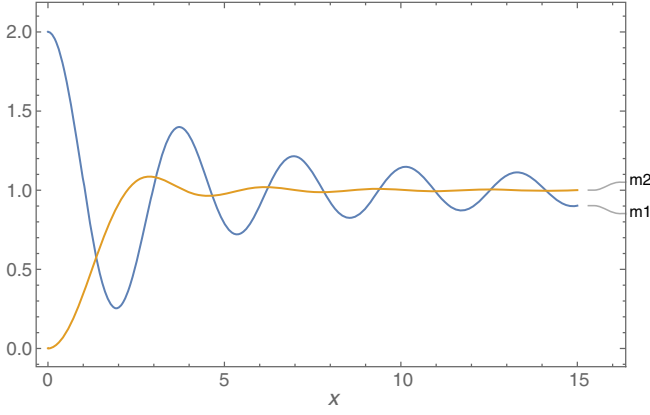


FIG. 1. Ratios  $m_1 = m_{\parallel}/m_0$  and  $m_2 = m_{\perp}/m_0$  as a function of the dimensionless  $x = a(|\nu| - \Omega)$  for Dirichlet boundary conditions on the mirror.

contrary, in the opposite regime, i.e., close to the plate, those functions approach rather different limits. Indeed,  $m_{\perp}$  is enhanced by a factor which approaches 2, that is  $m_{\perp}(\nu) \approx 2m_0(\nu)$ , while  $m_{\parallel}$  tends to zero in that limit. These results have a simple interpretation in terms of the images of the oscillating atom in each case.

### B. Neumann mirror

For a Neumann mirror, one has instead the propagator:

$$\begin{aligned} \langle \phi(x)\phi(y) \rangle_m &= G_0(x^0 - y^0, x^1 - y^1, x^2 - y^2, x^3 - y^3) \\ &+ G_0(x^0 - y^0, x^1 - y^1, x^2 - y^2, x^3 + y^3). \end{aligned} \quad (20)$$

Proceeding in an entirely analogous way as for the Dirichlet case,

$$\text{Im}[\Gamma_{mp}^N] = \frac{1}{2} \int_{-\infty}^{+\infty} \frac{d\nu}{2\pi} \tilde{y}^i(-\nu) \tilde{y}^j(\nu) m_N^{ij}(\nu). \quad (21)$$

where now the parallel component is

$$\begin{aligned} m_{\parallel}(\nu) &= \frac{\pi g^2}{2m\Omega} \theta(|\nu| - \Omega) \int \frac{d^3 p}{(2\pi)^3} \frac{\mathbf{P}_{\parallel}^2}{2p} [1 + \cos(2p^3 a)] \\ &\times \delta(|\nu| - p - \Omega), \end{aligned} \quad (22)$$

and results in

$$\begin{aligned} m_{\parallel}(\nu) &= \frac{g^2}{4\pi m\Omega} \theta(|\nu| - \Omega) (|\nu| - \Omega)^3 \\ &\times \left\{ \frac{1}{3} - \frac{\cos(2(|\nu| - \Omega)a)}{4[(|\nu| - \Omega)a]^2} + \frac{\sin(2(|\nu| - \Omega)a)}{8[(|\nu| - \Omega)a]^3} \right\}. \end{aligned} \quad (23)$$

The perpendicular component, on the other hand, is given by

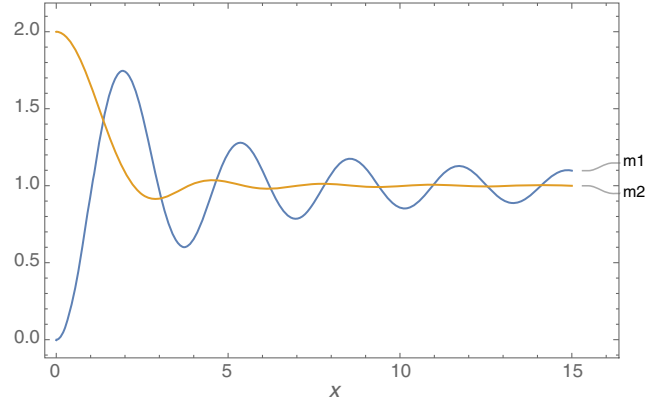


FIG. 2. Ratios  $m_1 = m_{\parallel}/m_0$  and  $m_2 = m_{\perp}/m_0$  as a function of the dimensionless  $x = a(|\nu| - \Omega)$  for Neumann boundary condition on the mirror.

$$\begin{aligned} m_{\perp}(\nu) &= \frac{\pi g^2}{2m\Omega} \theta(|\nu| - \Omega) \int \frac{d^3 p}{(2\pi)^3} \frac{(p^3)^2}{p} [1 - \cos(2p^3 a)] \\ &\times \delta(|\nu| - p - \Omega), \end{aligned} \quad (24)$$

or

$$\begin{aligned} m_{\perp}(\nu) &= \frac{g^2}{4\pi m\Omega} \theta(|\nu| - \Omega) (|\nu| - \Omega)^3 \\ &\times \left\{ \frac{1}{3} - \frac{\cos(2(|\nu| - \Omega)a)}{2[(|\nu| - \Omega)a]^2} \right. \\ &\left. + \frac{\sin(2(|\nu| - \Omega)a)}{4[(|\nu| - \Omega)a]^3} - \frac{\sin(2(|\nu| - \Omega)a)}{2[(|\nu| - \Omega)a]} \right\}. \end{aligned} \quad (25)$$

Far from the mirror, the results for Neumann boundary conditions also coincide with the free space case. Note, however, that the behaviors of  $m_{\parallel}$  and  $m_{\perp}$  close to the mirror are reversed, when compared with their Dirichlet counterparts. These results are illustrated in Fig. 2.

### III. TRANSITION AMPLITUDES

The existence of a threshold at  $|\nu| = \Omega$ , above which there is a continuum in frequency with a nonvanishing probability of vacuum decay, suggests that the processes involved correspond to an excitation of the electron in the atom (hence the threshold  $\Omega$ ), plus the emission of a massless scalar field particle (the continuum above the threshold). Besides, we know that the imaginary part of the effective action is related to the squared modulus of the transition amplitude for the creation of real particles, when the threshold is reached. To that end, and having in mind the calculation of the imaginary part of the effective action to the same order we have used, we consider the transition matrix  $T$ , related to the  $S$  matrix by  $S = I + iT$  ( $I$ : identity operator), to the lowest nontrivial order in the coupling constant  $g$ .

We use standard perturbation theory in the interaction representation, taking as free Hamiltonian the one corresponding to the free atom plus the free scalar field (including its boundary conditions). Therefore,

$$S = \mathbb{T} \exp \left\{ ig \int dt q(t) \phi[t, \mathbf{r}(t)] \right\}, \quad (26)$$

with  $\mathbb{T}$  the chronological ordering operator.

The matrix elements of the  $T$  matrix between the initial and final states, to the first order in  $g$ , are then of the form:

$$T_{fi} \equiv g \int dt \langle f | q(t) \phi[t, \mathbf{r}(t)] | i \rangle. \quad (27)$$

The operators above evolve independently, according to their respective free Hamiltonians, thus, for the electron degree of freedom:

$$q(t) = \frac{1}{\sqrt{2m\Omega}} (ae^{-i\Omega t} + a^\dagger e^{i\Omega t}), \quad (28)$$

where  $a$  and  $a^\dagger$  denote the standard destruction and creation operators for the harmonic oscillator. The scalar field, on the other hand, will have different expansions depending on whether the mirror imposes Dirichlet or Neumann boundary conditions. We consider these two alternatives below.

### A. Dirichlet plane

In this case, which we consider first, using the notations  $z \equiv x^3$ ,  $\mathbf{x}_\parallel \equiv (x^1, x^2)$  (and analogously for the components of  $\mathbf{k}$ ), we shall have

$$\phi(x) = \int d^2\mathbf{k}_\parallel \int_0^\infty dk_z [\alpha(\mathbf{k}) f_{\mathbf{k}}(x) + \alpha^\dagger(\mathbf{k}) f_{\mathbf{k}}^*(x)], \quad (29)$$

where

$$f_{\mathbf{k}}(x) = \frac{1}{\sqrt{4\pi^3 \omega(\mathbf{k})}} e^{-i\omega(\mathbf{k})t + i\mathbf{k}_\parallel \cdot \mathbf{x}_\parallel} \sin(k_z z), \quad (30)$$

$\omega(\mathbf{k}) = |\mathbf{k}|$  and the only nonvanishing commutator between the operators appearing in the decomposition is  $[\alpha(\mathbf{k}), \alpha^\dagger(\mathbf{k}')] = \delta(\mathbf{k} - \mathbf{k}')$ .

The initial state will be of the form  $|i\rangle = |0\rangle \otimes |0\rangle$ , where the first factor refers to the electron and the second one to the field. For this kind of initial state, the only nonvanishing contribution to  $T_{fi}$  will be of the form

$$|f\rangle = |1\rangle \otimes |\mathbf{k}\rangle, \quad |1\rangle \equiv a^\dagger |0\rangle, \quad |\mathbf{k}\rangle \equiv \frac{1}{\mathcal{N}} \alpha^\dagger(\mathbf{k}) |0\rangle. \quad (31)$$

The factor  $\frac{1}{\mathcal{N}}$  is included in order to normalize the state  $|\mathbf{k}\rangle$ , what is needed in order to obtain probabilities from  $T_{fi}^{(1)}$ . If the system is put in a cubic box of length  $L$ ,  $\mathcal{N} = \sqrt{\frac{L^3}{(2\pi)^3}}$ .

We find

$$T_{fi} = \frac{g}{\sqrt{m\Omega\omega(\mathbf{k})L^3}} \int_{-\infty}^{+\infty} dt e^{it(\Omega+\omega(\mathbf{k}))} e^{-i\mathbf{k}_\parallel \cdot \mathbf{r}_\parallel(t)} \times \sin[k_z r_z(t)]. \quad (32)$$

For parallel motion:  $r_z(t) \equiv a$ , and to the lowest non-trivial order in the departure  $\mathbf{y}_\parallel(t) = \mathbf{r}_\parallel(t)$ ,

$$T_{fi} \simeq -i \frac{g}{\sqrt{m\Omega|\mathbf{k}|L^3}} \sin(k_z a) \mathbf{k}_\parallel \cdot \tilde{\mathbf{y}}_\parallel (\Omega + |\mathbf{k}|). \quad (33)$$

Thus, the probability for the process, with the final particle in an infinitesimal volume in momentum space,  $dP_{fi}$ , is obtained by multiplying  $d^3\mathbf{k} |T_{fi}^{(1)}|^2$  by the density of final states:  $\frac{1}{2} \frac{L^3}{(2\pi)^3}$ . Note the factor of  $\frac{1}{2}$  with respect to the free space case, due to the fact that states with the third component of the momentum reversed are now identical.

Then

$$dP_{fi} = \frac{d^3\mathbf{k}}{(2\pi)^3} \frac{g^2}{2m\Omega k} \sin^2(k_z a) k^a k^b \times \tilde{y}^a(-(\Omega + k)) \tilde{y}^b(\Omega + k), \quad (34)$$

where  $a, b = 1, 2$ . It is convenient to introduce spherical coordinates centered at the mean position of the atom, such that  $\tilde{\mathbf{y}}$  is along the  $x^1$  axis. With this choice, the spatial dependence of the probability is explicitly given by

$$\begin{aligned} dP_{fi} &= \frac{g^2}{2(2\pi)^3 m\Omega} k^3 \sin^3 \theta \sin^2(ka \cos \theta) \cos^2 \varphi \\ &\times |\tilde{\mathbf{y}}_\parallel(\Omega + k)|^2 dk d\theta d\varphi \\ &\equiv \frac{g^2}{2(2\pi)^3 m\Omega} p_\parallel^D(ka, \theta, \varphi) |\tilde{\mathbf{y}}_\parallel(\Omega + k)|^2 k^3 \sin \theta dk d\theta d\varphi, \end{aligned} \quad (35)$$

where  $p_\parallel^D$  is proportional to the probability per unit solid angle. In Fig. 3 we plot this function for different values of the product  $ka$ . We see that for  $ka \leq O(1)$  the angular dependence corresponds to quadrupole radiation, as expected from the images method; indeed, in this regime the retardation between a wave emitted by the atom and the one due to its image can be ignored, and therefore the parallel oscillating dipole behaves as a quadrupole when combined with its image companion.

For intermediate values of  $ka$ , retardation cannot be ignored, and the angular dependence shows a complex structure of peaks, while at very large values  $\sin^2(ka \cos \theta)$  averages to  $1/2$ , the radiation becomes dipolar and coincides with that of an atom oscillating in free space.

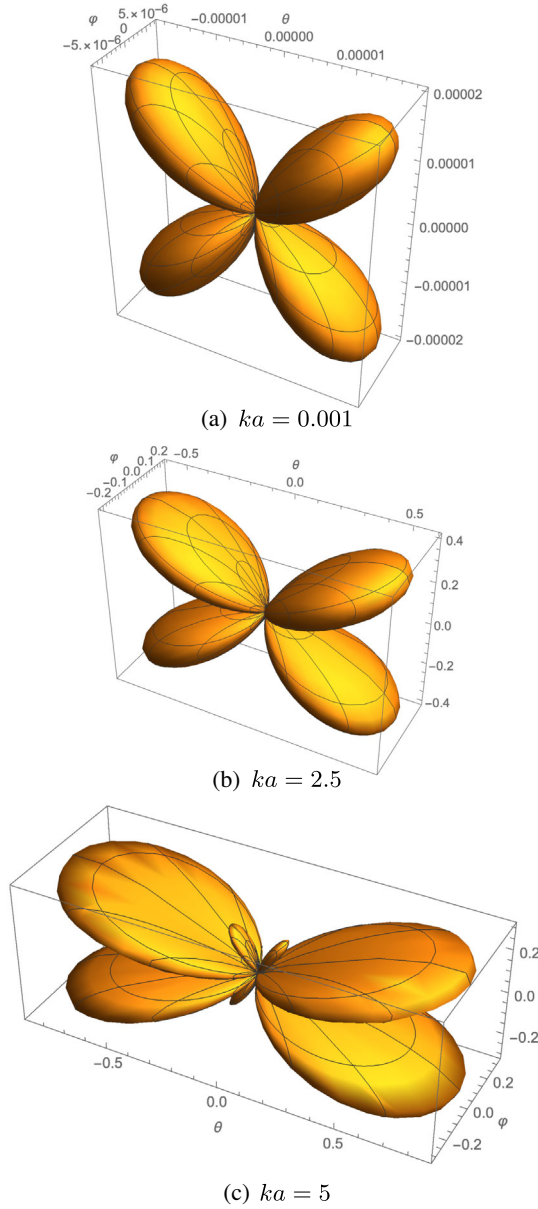


FIG. 3. We plot here  $p_{\parallel}^D$  from Eq. (36) as a function of spherical angles  $\theta$  and  $\varphi$ , for Dirichlet boundary condition and parallel motion.

The total probability of this kind of process  $P_{fi}$  is obtained by integrating out over all the possible momenta. Rather than integrating over the variables above, it is more convenient to proceed as follows:

$$\begin{aligned}
 P &= \int dP_{fi} \\
 &= \int d^3\mathbf{k} \int_{-\infty}^{\infty} d\nu \delta(|\nu| - \Omega - k) \frac{g^2}{2m\Omega k} \sin^2(k_z a) \\
 &\quad \times k^a k^b \tilde{y}^a(\nu) \tilde{y}^b(-\nu). \tag{36}
 \end{aligned}$$

Interchanging the order of the integrals, the one over  $\mathbf{k}$  may then be performed exactly. This produces an expression of the form

$$P = \frac{1}{2} \int \frac{d\nu}{2\pi} \rho_{\parallel}(\nu) |\tilde{y}(\nu)|^2. \tag{37}$$

$$\begin{aligned}
 \rho_{\parallel}(\nu) &= \frac{g^2}{4\pi m\Omega} \theta(|\nu| - \Omega) (|\nu| - \Omega)^3 \\
 &\quad \times \left\{ \frac{2}{3} + \frac{\cos(2(|\nu| - \Omega)a)}{2[ (|\nu| - \Omega)a ]^2} - \frac{\sin(2(|\nu| - \Omega)a)}{4[ (|\nu| - \Omega)a ]^3} \right\}. \tag{38}
 \end{aligned}$$

Note that this is in agreement with our results for the imaginary part, since  $P$  is twice the imaginary part of the effective action.

For motion perpendicular to the plane,

$$T_{fi} \simeq \frac{g}{\sqrt{m\Omega} |\mathbf{k}| L^3} \cos(k_z a) k_z \tilde{y}_{\perp}(\Omega + |\mathbf{k}|), \tag{39}$$

and

$$dP_{fi} = \frac{d^3\mathbf{k}}{(2\pi)^3} \frac{g^2}{2m\Omega k} \cos^2(k_z a) k_z^2 |\tilde{y}_{\perp}(\Omega + k)|^2. \tag{40}$$

In this case there is of course axial symmetry with respect to the direction of motion; therefore we may integrate the probability along  $\varphi$  angle

$$\begin{aligned}
 dP_{fi} &= \frac{g^2}{2(2\pi)^2 m\Omega} k^3 \sin\theta \cos^2\theta \cos^2(ka \cos\theta) \\
 &\quad \times |\tilde{y}_{\perp}(\Omega + k)|^2 dk d\theta \\
 &\equiv \frac{g^2}{2(2\pi)^2 m\Omega} p_{\perp}^D(ka, \theta) |\tilde{y}_{\perp}(\Omega + k)|^2 k^3 \sin\theta dk d\theta. \tag{41}
 \end{aligned}$$

In Fig. 4 and we plot the function  $p_{\perp}^D(ka, \theta)$  for different values of  $ka$ . We can see that the radiation has a dipolar pattern both at small and very large distances: at very small distances the image dipole reinforces (without retardation and therefore no interference) the effect of the vertical oscillating dipole associated to the moving atom, while at large distances we recover the result for the oscillating atom in free space.

Again, the total probability becomes identical to twice the imaginary part of the effective action (evaluated to the second order in  $g$ ).

In the same way, we shall study the spontaneous decay process in which the initial state is now given by  $|i\rangle = |1\rangle \otimes |0\rangle$  (i.e., the atom in the excited state and the field in vacuum) and the final state is given by  $|f\rangle = |0\rangle \otimes |1\rangle$ . It is straightforward to check that in this

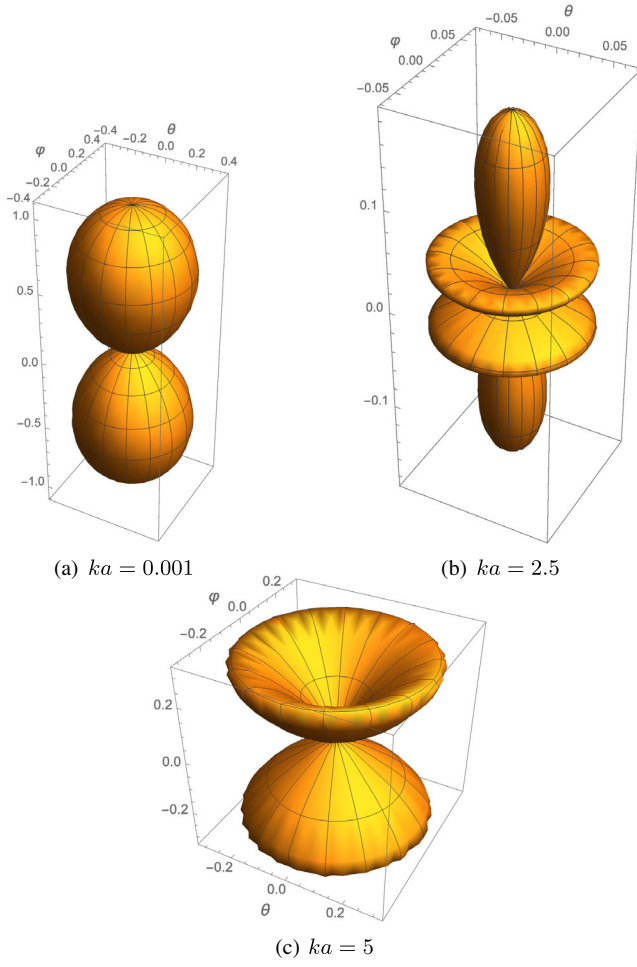


FIG. 4. We plot here  $p_{fi}^D$  from Eq. (42) as a function of spherical angles  $\theta$  and  $\varphi$ , for Dirichlet boundary condition and perpendicular motion.

case there is no threshold at  $|\nu| = \Omega$  and the result is given for the matrix element  $T_{fi}$  in the parallel motion is

$$T_{fi} = \frac{g}{\sqrt{m\Omega\omega(\mathbf{k})L^3}} \int_{-\infty}^{+\infty} dt e^{it(-\Omega+\omega(\mathbf{k}))} e^{-i\mathbf{k}_{\parallel}\cdot\mathbf{r}_{\parallel}(t)} \times \sin[k_z r_z(t)], \quad (42)$$

for  $r_z(t) \equiv a$ , and to the lowest nontrivial order in the departure  $\mathbf{y}_{\parallel}(t) = \mathbf{r}_{\parallel}(t)$ ,

$$T_{fi} \simeq \frac{g}{\sqrt{m\Omega|\mathbf{k}|L^3}} \sin[k_z a] [2\pi\delta(\Omega - \omega(k)) - i\mathbf{k}_{\parallel} \cdot \tilde{\mathbf{y}}_{\parallel}(-\Omega + |\mathbf{k}|)], \quad (43)$$

where, unlike the excitation case examined previously, there is a first term independent of the amplitude of the oscillation  $\tilde{\mathbf{y}}_{\parallel}$  that corresponds to the spontaneous decay for a static atom in front of a mirror. The probability for the decay process is now given by

$$dP_{fi} = \frac{d^3\mathbf{k}}{(2\pi)^3} \frac{g^2}{2m\Omega k} \sin^2(k_z a) [4\pi^2 T \delta(\Omega - |\mathbf{k}|) + k^a k^b \tilde{y}^a(-(-\Omega + |\mathbf{k}|)) \tilde{y}^b(-\Omega + |\mathbf{k}|)]. \quad (44)$$

For the motion perpendicular to the plane we have

$$T_{fi} \simeq \frac{g}{\sqrt{m\Omega|\mathbf{k}|L^3}} [2\pi\delta(\Omega - |\mathbf{k}|) \sin(k_z a) + k_z \tilde{y}_{\perp}(-\Omega + |\mathbf{k}|) \cos(k_z a)] \quad (45)$$

and

$$dP_{fi} = \frac{d^3\mathbf{k}}{(2\pi)^3} \frac{g^2}{2m\Omega k} [4\pi^2 T \delta(\Omega - |\mathbf{k}|) \sin^2(k_z a) + k_z^2 |\tilde{y}_{\perp}(-\Omega + |\mathbf{k}|)|^2 \cos^2(k_z a)], \quad (46)$$

assuming that  $\tilde{y}_{\perp}(0) = 0$ .

It is worth to remark that in both situations (parallel or perpendicular motions), if the atom's center of mass oscillates harmonically with a frequency  $\Omega_{\text{cm}} < \Omega$ , the spectrum of the emitted photons will have three different frequencies  $\omega = \Omega, \Omega \pm \Omega_{\text{cm}}$ . A similar phenomenon occurs for an atom in front of an oscillating mirror [6,7], in the adiabatic approximation. Only two frequencies would be present in the spectrum when  $\Omega_{\text{cm}} > \Omega$ .

## B. Neumann plane

We now have a different expansion for the field:

$$\phi(x) = \int d^2\mathbf{k}_{\parallel} \int_0^{\infty} dk_z [\alpha(\mathbf{k}) g_{\mathbf{k}}(x) + \alpha^{\dagger}(\mathbf{k}) g_{\mathbf{k}}^*(x)], \quad (47)$$

where

$$g_{\mathbf{k}}(x) = \frac{1}{\sqrt{4\pi^3|\mathbf{k}|}} e^{-i|\mathbf{k}|t + i\mathbf{k}_{\parallel}\cdot\mathbf{x}_{\parallel}} \cos(k_z z). \quad (48)$$

Since the interaction term is exactly the same as for the Dirichlet case, it is immediate to find the probabilities in this case. For parallel motion:

$$\begin{aligned} dP_{fi} &= \frac{g^2}{2(2\pi)^3 m\Omega} k^3 \sin^3\theta \cos^2(ka \cos\theta) \cos^2\varphi \\ &\quad \times |\tilde{\mathbf{y}}_{\parallel}(\Omega + k)|^2 dk d\theta d\varphi \\ &\equiv \frac{g^2}{2(2\pi)^3 m\Omega} p_{\parallel}^N(ka, \theta, \varphi) |\tilde{\mathbf{y}}_{\parallel}(\Omega + k)|^2 k^3 \\ &\quad \times \sin\theta dk d\theta d\varphi, \end{aligned} \quad (49)$$

while perpendicular departures are endowed with the probabilities

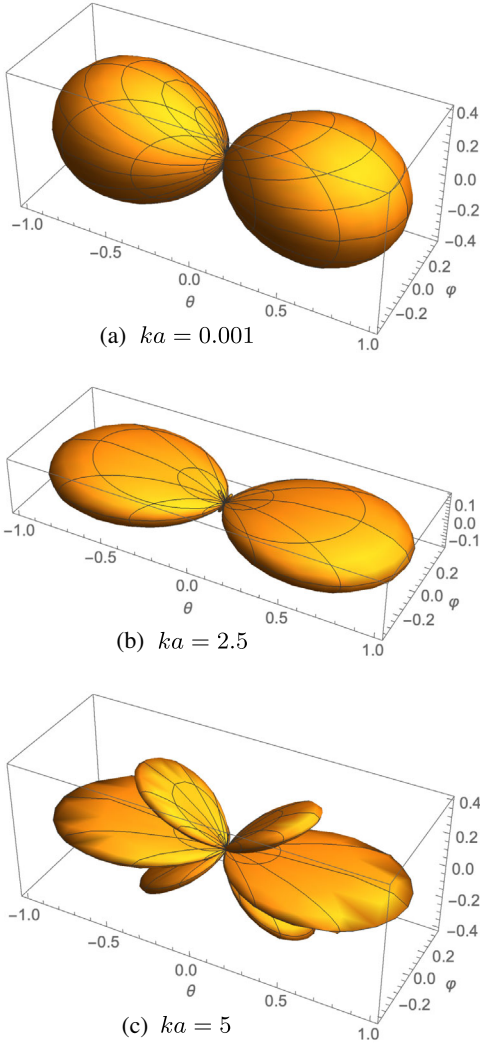


FIG. 5. We plot here  $p_{\parallel}^N$  from Eq. (49) as a function of spherical angles  $\theta$  and  $\varphi$ , for Neumann boundary condition and parallel motion.

$$\begin{aligned}
 dP_{fi} &= \frac{g^2}{2(2\pi)^2 m \Omega} k^3 \sin \theta \cos^2 \theta \sin^2(ka \cos \theta) \\
 &\quad \times |\tilde{y}_{\perp}(\Omega + k)|^2 dk d\theta \\
 &\equiv \frac{g^2}{2(2\pi)^2 m \Omega} p_{\perp}(ka, \theta) |\tilde{y}_{\perp}(\Omega + k)|^2 k^3 \sin \theta dk d\theta.
 \end{aligned} \tag{50}$$

In Figs. 5 and 6 we plot the function  $p_{\parallel}^N$  and  $p_{\perp}^N$ , respectively. Although less evident than in the Dirichlet case,  $p_{\perp}^N$  shows a quadrupole pattern at small distances, being proportional to  $\cos^4(\theta)$ .

Yet again, the total probabilities are consistent with the results obtained in the effective action approach.

For completeness we will study in this section the case of the spontaneous decay process with Neumann boundary

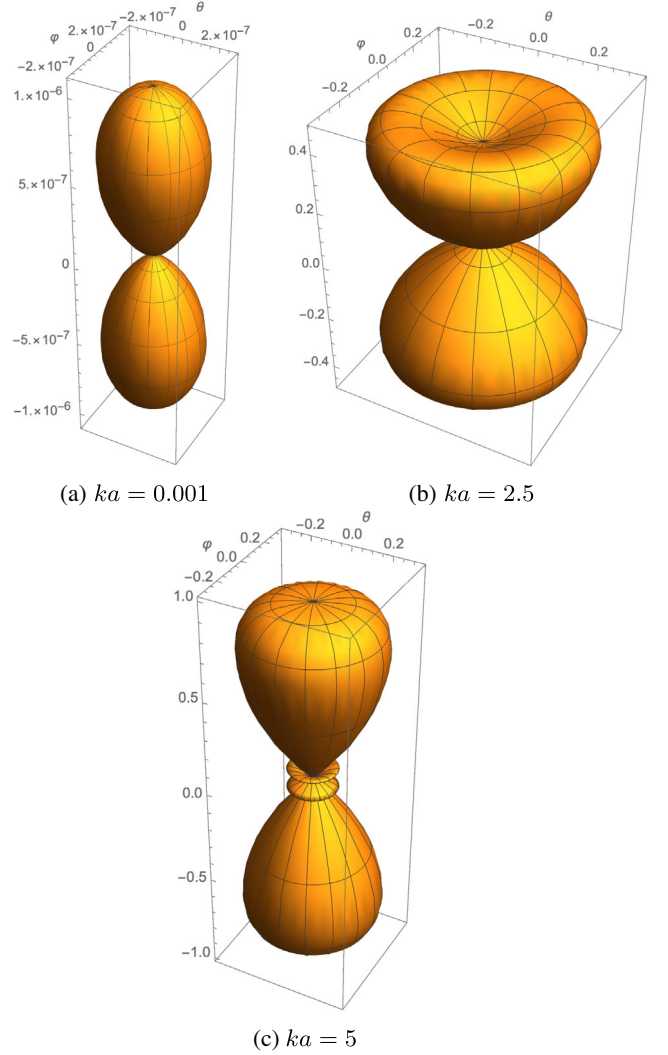


FIG. 6. We plot here  $p_{\perp}^N$  from Eq. (51) as a function of spherical angles  $\theta$  and  $\varphi$ , for Neumann boundary condition and perpendicular motion.

conditions on the perfect mirror. In the case of parallel to the plane oscillatory motion of the atom, the probability density for such process is obtained

$$\begin{aligned}
 dP_{fi} &= \frac{d^3 \mathbf{k}}{(2\pi)^3} \frac{g^2}{2m\Omega k} \cos^2(k_z a) [4\pi^2 T \delta(\Omega - k) \\
 &\quad + k^a k^b \tilde{y}^a(-(-\Omega + k)) \tilde{y}^b(-\Omega + k)].
 \end{aligned} \tag{51}$$

For the perpendicular motion we get

$$\begin{aligned}
 dP_{fi} &= \frac{d^3 \mathbf{k}}{(2\pi)^3} \frac{g^2}{2m\Omega k} [4\pi^2 T \delta(\Omega - k) \cos^2(k_z a) \\
 &\quad + k_z^2 |\tilde{y}_{\perp}(-\Omega + k)|^2 \sin^2(k_z a)].
 \end{aligned} \tag{52}$$

The spectrum of the emitted particles is similar to that of the Dirichlet plane. Note, however, that the dependence with

the mean distance to the mirror is different, as well as the relative weight between the static and nonstatic contributions for the case of perpendicular motion.

#### IV. CONCLUSIONS

In this paper we have studied the phenomena of excitation and spontaneous emission of a moving atom in front of a perfect mirror, in a model where the atom is coupled to a quantum real scalar field, and the perfect conductor boundary conditions have been mimicked by Dirichlet and Neumann boundary conditions.

Assuming that the atom performs small amplitude motions, we computed the vacuum decay probability to the second order in the coupling constant between the electron and the field. This probability is determined by the imaginary part of the effective action, which is a functional of the trajectory of the atom's center of mass. When the atom is close enough to the mirror, the results for Dirichlet and Neumann boundary conditions admit simple interpretations in terms of the images method.

The physical process behind vacuum decay is, up to this order, the transition of the atom from the ground state to the first excited state, along with the emission of a photon. Thus, there is a threshold for the process dictated by energy conservation which is  $\Omega_{cm} > \Omega$ . We have also computed the probability for the decay process as a function of the direction of the emitted particle, and checked that the integration over all directions reproduce the vacuum decay probability. The angular dependence of the probability can also be understood in terms of the images

method. In particular, for Dirichlet boundary conditions, the radiation emitted by an atom in parallel motion becomes quadrupolar when the atom is close to the mirror. For Neumann boundary conditions this happens for perpendicular motion.

Finally, we analyzed the spontaneous decay of an oscillating atom in front of a mirror. Both the presence of the mirror and the oscillation of the atom induce corrections to the spontaneous emission in free space. The presence of the mirror modifies the angular dependence of the probability, that turns out to be a function of the atom-mirror distance, but not the energy of the emitted photons. When the atom oscillates, the spectrum of the emitted particles is modified by the appearance of two lateral peaks, symmetric with respect to the central peak that corresponds to the static atom. These results are similar to those for a static atom in front of an oscillating mirror, and opens new possibilities for the eventual experimental observation of the effect. The extension of our results to the more realistic case of the electromagnetic field can be addressed, in the dipole approximation, using similar techniques. Work in this direction is in progress.

#### ACKNOWLEDGMENTS

This research was supported by Agencia Nacional de Promoción Científica y Tecnológica (ANPCyT), Consejo Nacional de Investigaciones Científicas y Técnicas (CONICET), Universidad de Buenos Aires (UBA), and Universidad Nacional de Cuyo (UNCuyo).

- 
- [1] P. W. Milonni, *The Quantum vacuum: An Introduction to quantum electrodynamics* (Academic Press, San Diego, CA, USA, 1994); K. A. Milton, *The Casimir Effect: Physical Manifestations of Zero-Point Energy* (World Scientific, River Edge, NJ, USA, 2001); M. Bordag, G. L. Klimchitskaya, U. Mohideen, and V. M. Mostepanenko, *Advances in the Casimir Effect* (Oxford University Press, Oxford, UK, 2009).
- [2] H. Walther, B. T. H. Varcoe, B. G. Englert, and T. Becker, *Rep. Prog. Phys.* **69**, 1325 (2006).
- [3] V. V. Dodonov, *Phys. Scr.* **82**, 038105 (2010); D. A. R. Dalvit, P. A. M. Neto, and F. D. Mazzitelli, *Lect. Notes Phys.* **834**, 419 (2011); P. D. Nation, J. R. Johansson, M. P. Blencowe, and F. Nori, *Rev. Mod. Phys.* **84**, 1 (2012); V. V. Dodonov, *Physics* **2**, 67 (2020).
- [4] R. de Melo e Souza, F. Impens, and P. A. M. Neto, *Phys. Rev. A* **97**, 032514 (2018).
- [5] L. Lo and C. K. Law, *Phys. Rev. A* **98**, 063807 (2018); L. Lo, P. T. Fong, and C. K. Law, *Phys. Rev. A* **102**, 033703 (2020).
- [6] A. W. Glaetzle, K. Hammerer, A. J. Daley, R. Blatt, and P. Zoller, *Opt. Commun.* **283**, 758 (2010).
- [7] A. Ferreri, M. Domina, L. Rizzuto, and R. Passante, *Symmetry* **11**, 1384 (2019).
- [8] B. P. Dolan, A. Hunter-McCabe, and J. Twamley, *New J. Phys.* **22**, 033026 (2020).
- [9] A. A. Svidzinsky, J. S. Ben-Benjamin, S. A. Fulling, and D. N. Page, *Phys. Rev. Lett.* **121**, 071301 (2018).
- [10] M. B. Farías, C. D. Fosco, F. C. Lombardo, and F. D. Mazzitelli, *Phys. Rev. D* **100**, 036013 (2019).
- [11] C. D. Fosco, F. C. Lombardo, and F. D. Mazzitelli, *Universe* **7**, 158 (2021).